



Optical monitoring observations of two γ -ray narrow-line Seyfert 1 galaxies



Hao Liu^{a,b,*}, Chao Wu^a, Jing Wang^a, Jianyan Wei^a

^a Key Laboratory of Space Astronomy and Technology, National Astronomical Observatories, Chinese Academy of Sciences, 20A Datun Road Chaoyang District, Beijing 100012, P.R.China

^b University of Chinese Academy of Sciences, Shijingshan District, Beijing 100049, P.R.China

HIGHLIGHTS

- Optical observations for 2 γ -ray NLS1s were carried out in B and R bands.
- Difference image subtraction was used for the extended host galaxy of 1H 0323+342.
- Variability on day timescale were observed for 1H 0323+342.
- INOV was confirmed for SDSS J094857.3+002225.
- Microvariability indicated the existence of a relativistic jet in these NLS1s.

ARTICLE INFO

Article history:

Received 9 April 2015

Revised 6 August 2015

Accepted 18 September 2015

Available online 26 September 2015

Communicated by G. Brunetti

Keywords:

Galaxies: active

Galaxies: jets

Galaxies: photometry

Galaxies: Seyfert

ABSTRACT

1H 0323+342 is a rather radio-loud narrow-line Seyfert 1 galaxy (NLS1) with γ -ray emission. Optical observations were carried out in B and R bands which covered 6 nights in 2011 to obtain light curves of 1H 0323+342. The difference image subtraction method was used to deal with the data of 1H 0323+342 because of the existence of extended host galaxy. Optical variability on day timescale was reported here. We also monitored the first γ -ray NLS1 SDSS J094857.3+002225 and confirmed the existence of intranight optical variability (INOV). These indicated the existence of a relativistic jet in these NLS1s.

© 2015 Elsevier B.V. All rights reserved.

1. Introduction

Narrow-line Seyfert 1 galaxies (NLS1s) are a peculiar and interesting class of active galactic nuclei (AGNs) with unusually narrow permitted lines (Osterbrock and Pogge, 1985). There are some classification criteria for NLS1s as (Osterbrock and Pogge, 1985; Goodrich, 1989; Pogge, 2000): (1) the narrow permitted lines only slightly broader than the forbidden lines; (2) $[O\ III]/H\beta < 3$, but exceptions are allowed if there is also strong $[Fe\ VII]$ and $[Fe\ X]$ present, unlike what is seen in Seyfert 2s; (3) the full widths at half-maximum (FWHM) of the $H\beta$ line $< 2000\ km\ s^{-1}$. Furthermore, strong Fe II emission lines or higher ionization iron lines can often be observed in NLS1s (Osterbrock and Pogge, 1985; Goodrich, 1989). They usually show steeper spectra and rapid variability in the X-ray regime

(Boller et al., 1996; Boller, 1997; Leighly, 1999; Malizia et al., 2008; Panessa et al., 2011). Usually, they are considered as objects with small black hole masses and very high Eddington ratios (Boller et al., 1996; Boroson, 2002; Grupe and Mathur, 2004).

NLS1s show remarkable radio-loud/radio-quiet dichotomy. It is not surprising that NLS1s are usually found radio-quiet, for they are considered as AGNs with small black hole masses and high accretion rates (Laor, 2000; Ho, 2002; Greene et al., 2006). However, a small part (about 7%) of them are radio-loud ($R > 10$) (Zhou and Wang, 2002; Komossa et al., 2006; Whalen et al., 2006; Zhou et al., 2006), where the radio loudness R is usually defined as the flux ratio of radio to optical at $\lambda 4400$ (Kellermann et al., 1989). The very radio-loud ($R > 100$) NLS1s are even less ($\sim 2.5\%$) (Komossa et al., 2006). Radio-loud NLS1s make up of an attractive and special group of AGNs.

The origin of radio-loud NLS1s (RL-NLS1s) has not been clearly understood. Several scenarios, considered the beaming effect (Remillard et al., 1991; Wang et al., 2001; Padovani et al., 2002; Zhou et al., 2003; 2005), accretion mode (e.g., Collin and Kawaguchi, 2004; Heinzeller and Duschl, 2007; Sikora et al., 2007), black hole mass and black hole

* Corresponding author at: Key Laboratory of Space Astronomy and Technology, National Astronomical Observatories, Chinese Academy of Sciences, 20A Datun Road, Chaoyang District, Beijing 100012, P. R. China. Tel.: +8613811935480; fax: +861064806323.

E-mail address: liuh@bao.ac.cn (H. Liu).

<http://dx.doi.org/10.1016/j.newast.2015.09.005>

1384-1076/© 2015 Elsevier B.V. All rights reserved.

spin (e.g., Blandford and Znajek, 1977; Blandford and Payne, 1982; Mathur and Grupe, 2005), for example, have been suggested to explain the sparseness of RL-NLS1s (see Komossa et al., 2006; Yuan et al., 2008). Some RL-NLS1s show interesting broadband properties which are unusually similar to those of blazars (Zhou et al., 2003; 2005; 2007; Gallo et al., 2006; Yuan et al., 2008). Some of them show flat spectra and blazar-like spectral energy distributions (SEDs) (Gallo et al., 2006; Zhou et al., 2006; Yuan et al., 2008). They also have high brightness temperatures which indicate the presence of relativistic jets (Zhou et al., 2003; Yuan et al., 2008; Abdo et al., 2009a).

The Large Area Telescope (LAT) onboard *Fermi Gamma-ray Space Telescope* (hereafter *Fermi*) discovered high-energy γ -ray emission from a RL-NLS1 SDSS J094857.3+002225 (Abdo et al., 2009a; Abdo et al., 2009b; Foschini et al., 2010). Soon, three new γ -ray-emitting RL-NLS1s were detected with *Fermi/LAT* (Abdo et al., 2009c). Foschini et al. (2011) reported more *Fermi/LAT* detections of γ -ray NLS1s, leading the number of detected γ -ray NLS1s to 7. Later, Eggen et al. (2014) reported two more γ -ray-emitting RL-NLS1s. Some of them have shown significant γ -ray flux variations (Calderone et al., 2011; Paliya et al., 2015). The γ -ray variability on timescale of several days supports the presence of a relativistic jet (Calderone et al., 2011). The variability and average photon indices are similar to those of flat spectrum radio quasars (FSRQs) (Paliya et al., 2015). Blazars and radio galaxies were known as two types of γ -ray AGNs. γ -ray-emitting RL-NLS1s above could be considered as a new class of γ -ray AGNs (Abdo et al., 2009c; Foschini et al., 2010).

Optical observations could provide important information about the AGN, for instance, the physical scales and structures of the engines (Webb and Malkan, 2000). The presence of relativistic jets suggests us to search for the intraday optical variability in those γ -ray RL-NLS1s for the relativistic beaming effect (Wagner and Witzel, 1995; Stalin et al., 2004). If these γ -ray NLS1s indeed host relativistic jets beaming towards our lines of sight, intraday variability should be detected. Liu et al. (2010) first discovered violent intranight optical variability (INOV) on the timescale of several hours and suggested the existence of a relativistic jet in SDSS J094857.3+002225. Later, more extreme optical variabilities on timescales ranging from minutes to years were observed in the same object (Maune et al., 2011; 2013; Paliya et al., 2013). Rapid optical variations were also detected in RL-NLS1s J1305+5116 (Maune et al., 2011) and PKS 1502+036 (Paliya et al., 2013). INOV was also detected in RL-NLS1 1H 0323+342, which indicated the presence of relativistic jets in the object (Paliya et al., 2013). However, it should be emphasized that aperture photometry was used to get the light curves in this work, while extended host galaxy has been detected in 1H 0323+342.

1H 0323+342 and SDSS J094857.3+002225 are two γ -ray RL-NLS1s which could be right candidates for searching for intraday variability. For the nearby one 1H 0323+342, although it is brighter, the contamination of the host galaxy should be considered (Zhou et al., 2007; Antón et al., 2008; León Tavares et al., 2014). In this work, we will introduce our effort on observations of these two γ -ray RL-NLS1s at optical band, including the attempt of plotting a light curve of 1H 0323+342 blended with extended host galaxy, and the farther monitoring of SDSS J094857.3+002225.

These two sources are introduced in Section 2. The observations and data reduction are presented in Section 3. The results are presented in Section 4. We presented our discussion in Section 5 and summarized conclusions in Section 6.

2. 1H 0323+342 and SDSS J094857.3+002225

1H 0323+342. The γ -ray detected object is identified as a NLS1 due to its small Balmer line width (about 1600 km s^{-1}), small $[O III]/H\beta$ of about 0.12, strong optical Fe II complexes and evident X-ray excess (Zhou et al., 2007; Foschini et al., 2009). Radio observations indicate that it is a strong radio source with an 8 GHz radio power

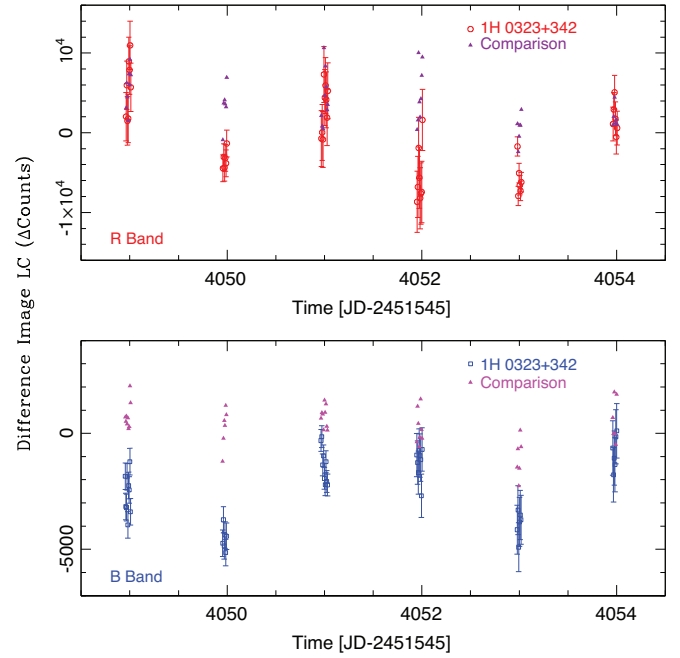


Fig. 1. Difference image residual flux light curves of 1H 0323+342 on the nights of 2011 February 1–6. The top and bottom panels give curves of R and B bands, respectively. The red open circles and blue open squares represent the residual flux of 1H 0323+342 in R and B band, respectively. The purple and magenta filled triangles represent the residual flux of comparison stars in R and B band, respectively. (For interpretation of the references to colour in this figure legend, the reader is referred to the web version of this article).

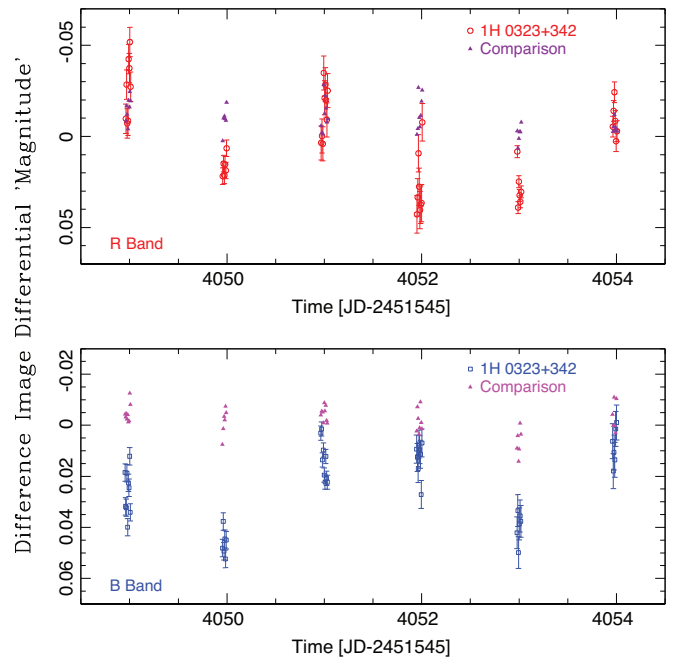


Fig. 2. Differential "magnitude" curves of 1H 0323+342 on the nights of 2011 February 1–6, which were obtained using the difference image subtraction method. The top and bottom panels give differential "magnitude" of R and B bands, respectively. The red open circles and blue open squares represent the differential "magnitude" of 1H 0323+342 in R and B band, respectively. The purple and magenta filled triangles represent the difference image differential "magnitude" of comparison stars in R and B band, respectively. (For interpretation of the references to colour in this figure legend, the reader is referred to the web version of this article).

of $10^{24.6}$ W Hz $^{-1}$ (Wajima et al., 2014), which results in an extreme observed radio loudness ($\log R = 2.39$) (Doi et al., 2012). Blazar-like properties are additionally revealed in the object: (1) a compact core-jet structure (Zhou et al., 2007; Wajima et al., 2014) with a flat spectral index $\alpha_r \approx 0.1$ ($S_\nu \propto \nu^\alpha$) (Neumann et al., 1994); (2) a relativistic jet beaming towards observers as suggested by its high brightness temperature ($> (5.2 \pm 0.3) \times 10^{10}$ K) (Wajima et al., 2014). Significant variations have been observed in the object in radio, X-ray and γ -ray bands (Zhou et al., 2007; Wajima et al., 2014; Paliya et al., 2014; 2015; Yao et al., 2015). Wajima et al. (2014) reported the short-term radio variability in 1H 0323+342 on a timescale of 1 month, which might be associated with the γ -ray-emitting region. Finally, it is emphasized that the object is a rather nearby object at $z = 0.063$, whose optical magnitude is $V = 15.72$ mag (Véron-Cetty and Véron, 2010). It was suggested that 1H 0323+342 was located in the host one-armed spiral structure or ring-structure, which might be a remnant of an interaction (Zhou et al., 2007; Antón et al., 2008; León Tavares et al., 2014).

SDSS J094857.3+002225. The FWHM of H β of the first γ -ray detected NLS1 SDSS J094857.3+002225 is rather narrow, about 1500 km s $^{-1}$ (Zhou et al., 2003; Yuan et al., 2008). Komossa et al. (2006) suggested that its mass of black hole is $4 \times 10^7 M_\odot$. It is a very radio-loud NLS1 at $z = 0.585 \pm 0.001$, whose radio loudness R is more than 1000 (Zhou et al., 2003; Komossa et al., 2006; Yuan et al., 2008; Abdo et al., 2009a). Its radio spectrum is flat and inverted (Zhou et al., 2003; Healey et al., 2007; Abdo et al., 2009a). Its brightness temperature was suggested to be very high ($\geq 10^{13}$ K

(Zhou et al., 2003). The SEDs modeling and variability indicate that the jet hosted by it is similar to those hosted by FSRQs (Foschini et al., 2012). Abdo et al. (2009b) suggested that its calculated power was within the average range of blazar powers. In addition, the observations of the variable polarization at about 18.8% provided useful information of the relativistic jet scenario (Ikejiri et al., 2011; Eggen et al., 2013; Itoh et al., 2013). SDSS J094857.3+002225 has been noticed to be variable at different wavelengths from radio to γ -ray (Abdo et al., 2009b; Foschini et al., 2012). Radio variations on different timescales ranging from weeks to years were reported (Zhou et al., 2003; Abdo et al., 2009b; Foschini et al., 2012). On optical bands, it also shows variability on long (Zhou et al., 2003) and shorter timescales (Abdo et al., 2009b). The discovery of its intranight optical variability made it be the first discovered RL-NLS1 with INOV, which provided evidence of the existence of a relativistic jet (Liu et al., 2010). Then more observations of its optical variability on timescales ranging from minutes to years were reported (Maune et al., 2013; Eggen et al., 2013; Paliya et al., 2013). It also varies in the X-ray and γ -ray bands on long and short timescales (Abdo et al., 2009b; Calderone et al., 2011; Foschini et al., 2012; Paliya et al., 2015).

3. Observations and data reduction

The observations of these two NLS1s in the Johnson B and R bands were carried out at the Xinglong Observatory of National Astronomical Observatories, Chinese Academy of Sciences (NAOC). The observations were obtained with two different telescopes, the 80 cm TNT

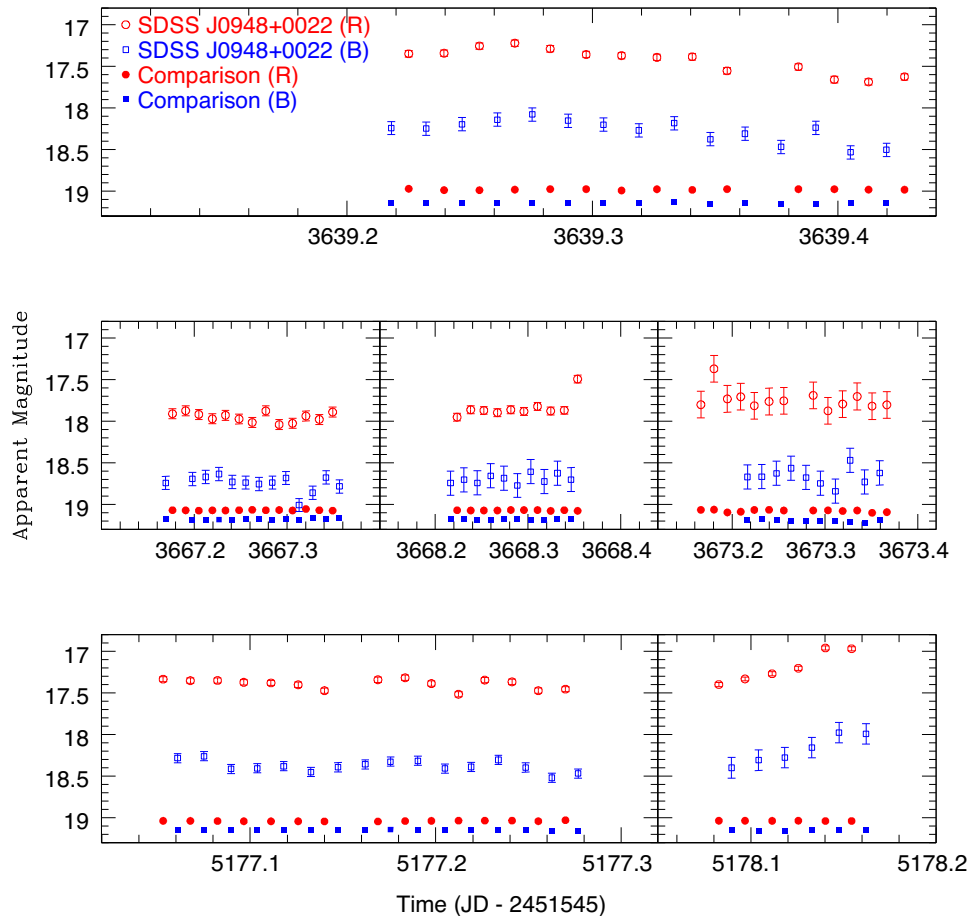


Fig. 3. Differential light curves for SDSS J094857.3+002225. The upper, middle and lower panels give curves obtained on the nights of December 18, 2009, January 15, 16, 21, 2010, and March 5 and 6, 2014, respectively. The red open circles and blue open squares represent the apparent magnitude of SDSS J094857.3+002225 in R and B bands, respectively. The red filled circles and blue filled squares represent the apparent magnitude of comparison stars in R and B bands, respectively. The points of the comparison stars have been shifted vertically for proper display. (For interpretation of the references to colour in this figure legend, the reader is referred to the web version of this article).

telescope (Tsinghua-NAOC Telescope) and the 2.16 m telescope. The 80 cm TNT telescope is a Cassegrain system with a $f/10$ beam (Huang et al., 2012). A liquid nitrogen cooled PI VA1300B 1300×1340 LN CCD which covers $\sim 11 \times 11$ arcmin² of the sky is used as the detector of the 80 cm telescope. Each pixel corresponds to $\sim 0.5 \times 0.5$ arcsec². The gain of the CCD is 2.3 electrons ADU⁻¹. The readout noise is 5 electrons. Additionally, the BAO Faint Object Spectrograph and Camera (BFOSC) system mounted at $f/9$ Cassegrain focus of the 2.16 m R-C (Ritchey Chretien) optical telescope was also used to carry out the observations (Yao et al., 2002). A liquid nitrogen cooled E2V CCD55-30 CCD with 1242×1152 pixels is used as the detector of the 2.16 m telescope. The entire CCD chip covers 9.46×8.77 arcmin² of the sky, whose each pixel corresponds to 0.457×0.457 arcsec² of the sky. The gain and readout noise of this CCD is 1.08 electrons ADU⁻¹ and 2.54 electrons, respectively.

The sky flat-field images in both *B* and *R* bands were obtained during the twilight time before and after each observation. The dark electrons could be entirely ignored because of the rather low temperature of the liquid nitrogen cooled CCD detector. Thus, dark frames are not needed for observations obtained with both telescopes.

Image pre-processing such as bias subtraction and flat-field corrections were done through standard routines by IRAF package¹.

3.1. 1H 0323+342

For the γ -ray NLS1 1H 0323+342, considered the contamination of the extended host galaxy, difference image subtraction method was used to obtain the light curve (Choi et al., 2014). The observations were carried out using the 2.16 m telescope on 6 moonless nights of February 1–6, 2011. The typical exposure time is 240–300 s for each frame.

The image pre-processing had been done through IRAF as above. Considering the slight different centers and orientation of the images, we performed astrometric transform to match the coordinates of all the frames using IRAF. A deeper, coadded template frame was made from the observed images. The template image was convolved with a space-varying kernel to match the observing conditions of the observed image. Thus, the convolved template was subtracted from the observed image to obtain the difference image. More details about the image subtraction could be found in works of Alard and Lupton (1998) and Alard (2000).

Forced aperture photometry routine was performed to measure the residual flux of the object in each difference image through IRAF (Choi et al., 2014). The residual fluxes for each object are summed within three apertures of 4, 6 and 8 pixels. Considering the atmospheric seeing and the attempt of aperture photometry, we chose 8 pixels as the aperture. The sum of residual fluxes was divided by the sum of the PSF matching kernels to make each difference image to be comparable to each other. Then, the residual fluxes from different frames could be compare together. Choi et al. (2014) argued that the difference image light curves (LCs) were very reasonable for AGN variability study. The difference image LCs showed the same fluctuation pattern with the photometric LCs. It has been found that the difference image LCs reproduce their corresponding photometric LCs very well (Choi et al., 2014). Thus, the difference image LCs could reveal the variability of the AGN with surrounding host galaxy.

Several steady stars with comparable brightness with the object were used as check stars to get the error bars. Image subtraction technique was also used to get the difference image light curve of the check stars. The error bars of the source are estimated from the average amplitude of variation of these check stars.

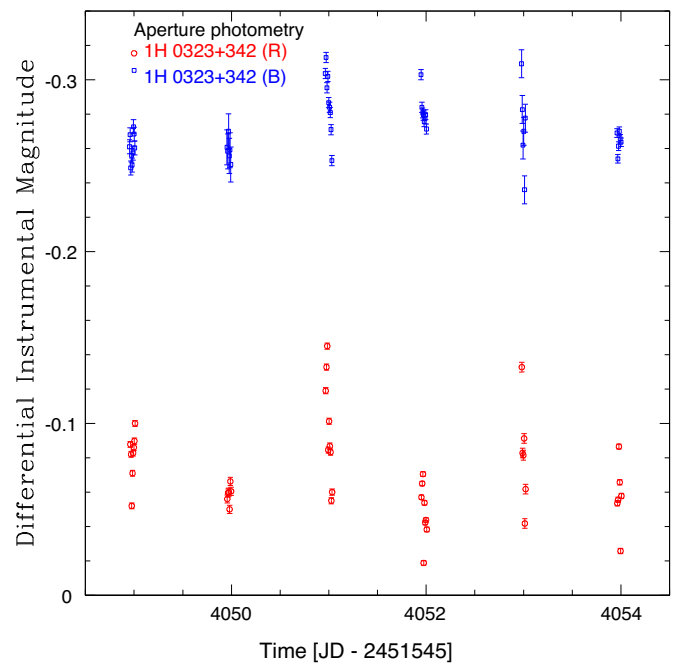


Fig. 4. Differential light curves for 1H 0323+342 on the nights of 2011 February 1–6, using forced aperture photometry directly. This figure was prepared by processing the observations with the method by Paliya et al. (2013). The red open circles and blue open squares represent the forced aperture photometry differential instrumental magnitude of 1H 0323+342 in the R and B bands, respectively. (For interpretation of the references to colour in this figure legend, the reader is referred to the web version of this article).

3.2. SDSS J094857.3+002225

The γ -ray RL-NLS1 SDSS J094857.3+002225 was monitored using the 80 cm TNT telescope on several moonless nights. In detail, the observations were carried out on the nights of December 18, 2009, January 15, 16, 21, 2010, and March 5 and 6, 2014. Continuous observations were carried out as long as possible to get more information on short timescales. The typical exposure time is about 600 s for each frame to get images with enough signal-to-noise ratio.

Several comparison stars were selected from the same CCD frame to obtain the differential magnitudes. The intrinsic brightness of the comparison stars could be obtained² from the database of the Sloan Digital Sky Survey (SDSS). Usually, the fluctuations of the comparison stars are not larger than 0.05 mag. In order to assess the errors, several check stars whose brightness is comparable to the brightness of the object were selected, while the comparison stars are brighter than the source. As the source is point-like without extended emission, standard aperture photometry routine APPHOT task of IRAF was adopted to get the instrumental magnitudes. Then we calculated the differential light curve of the source. The relation between the instrumental magnitudes and FWHM has also been analyzed and no correlation has been found. The FWHM of the source is comparable to those of the field stars in each frame. Thus, the circular aperture radius we adopted is twice of the mean FWHM of the field stars.

4. Results

4.1. 1H 0323+342

Residual fluxes of 1H 0323+342 and check stars were obtained using image subtraction technique. The difference image LCs are free of host galaxy contamination. Only the variable nuclei will stand out

¹ IRAF is distributed by the National Optical Astronomy Observatory, which is operated by the Association of Universities for Research in Astronomy, Inc., under cooperative agreement with the National Science Foundation; <http://iraf.noao.edu>.

² <http://www.sdss.org/dr6/algorithms/sdssUBVRITransform.html#Lupton2005>.

(Choi et al., 2014). The fluctuations of the check stars are not larger than 0.02 mag in both B and R band. The light curve of residual flux is plotted in Fig. 1. In Fig. 1, the fluctuation amplitude of residual flux of the object on one night is similar to those of check stars. Considering the fluctuation of residual flux between different days, it could be found that its fluctuation is larger than those of check stars on the timescale of several days. It is implied that we did not find intranight variability of this source on the timescale of several hours for the check stars are unchangeable. Besides, it is indicated that optical variability on day timescale of 1H 0323+342 was found on our campaign.

Although the exact flux of the AGN on the template frame is unknown because of the contamination of the extended host galaxy, the order of the flux could be estimated. Then, we could estimate the amplitude of the variation. Considering the differential magnitude:

$$m_1 - m_0 = -2.5 \lg (E_1 / E_0), \quad (1)$$

where the E_1, E_0 are the detected illuminations of stars, the differential magnitude could be described as:

$$m_1 - m_0 = -2.5 \lg (\Delta E / E_0 + 1), \quad (2)$$

where $\Delta E = E_1 - E_0$.

The flux within the photometry radius of the template could be used as the approximate flux of the object. Considering the host galaxy contamination, only a part of the flux detected within the aperture was actual contributed by the object. We used 50% as the

coefficient to get the order of the flux of 1H 0323+342. Then, the differential variation could be estimated using Eq. 2. We plotted the light curve of differential “magnitudes” of 1H 0323+342 in Fig. 2. In Fig. 2, the intranight fluctuation amplitude of 1H 0323+342 and check stars are similar with each other, while the check stars are unchangeable whose fluctuations are not larger than 0.02 mag using aperture photometry. Considering the fluctuation between different days, its fluctuation of the differential “magnitudes” is larger than those of check stars. For example, the differences between the mean “magnitudes” of 1H 0323+342 on Feb 2 and Feb 3, 2011 (the corresponding dates on the time-axis of Fig. 2 are 4050 and 4051) are about 0.032 and 0.031 “magnitudes” in B and R band, respectively. The errors are about 0.003 and 0.009 “magnitudes” in B and R band, respectively. Considered the criteria C parameter (Jang and Miller, 1997), the variability of 1H 0323+342 on day timescale is believable. Thus, as the differential “magnitudes” shown in the figures, although no significant intranight optical variability has been found, it is indicated that the γ -ray NLS1 1H 0323+342 has been detected variable on day timescale. The variability on day timescale also provides evidence supporting the existence of a relativistic jet in 1H 0323+342.

4.2. SDSS J094857.3+002225

The observations of object SDSS J094857.3+002225 could be divided into 3 parts. Each part contains about one week. The apparent magnitudes of the source could be calculated with the differential

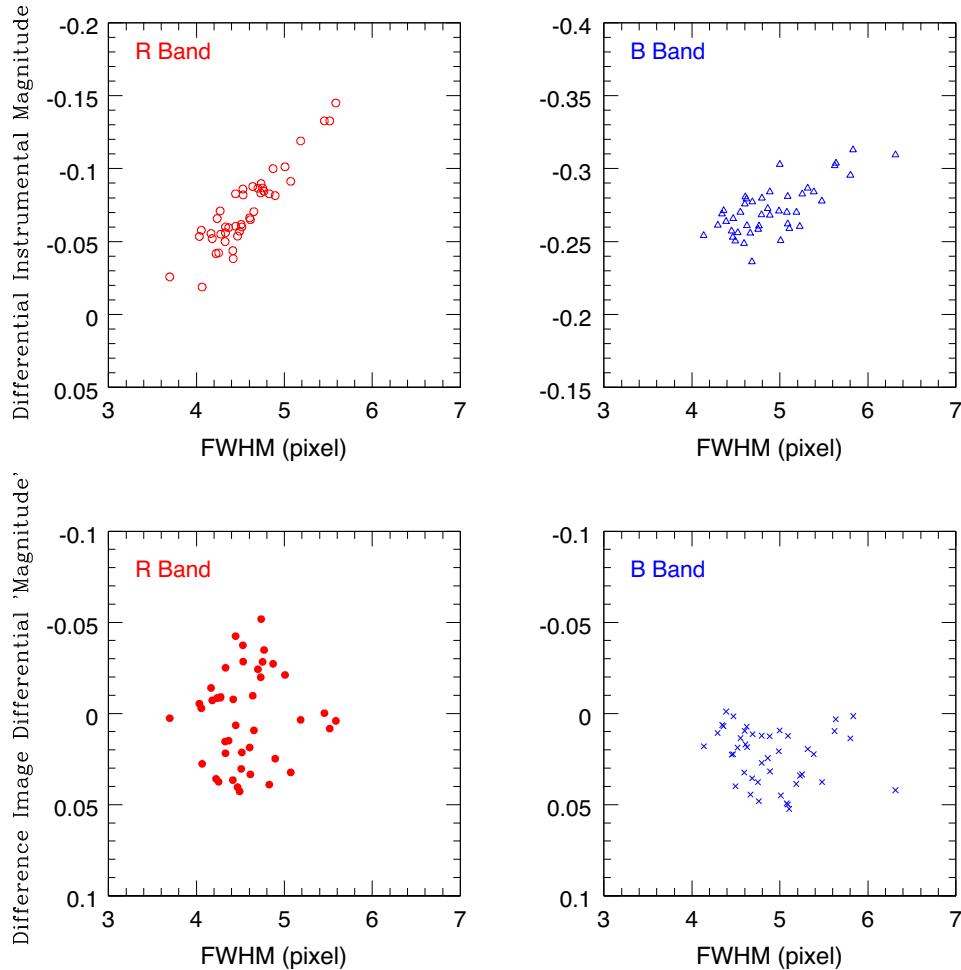


Fig. 5. Top panels: the relation between forced aperture photometry differential magnitude of 1H 0323+342 and FWHM. Bottom panels: the relation between difference image subtraction differential “magnitude” of 1H 0323+342 and FWHM. Top left and top right panels show relations of differential magnitude and FWHM in R and B bands, respectively. Bottom left and bottom right panels give relations of differential “magnitude” and FWHM in R and B bands, respectively.

magnitudes and the information of the comparison stars. The fluctuations of the comparison stars are usually not larger than 0.05 mag. Light curve of the observations are plotted in Fig. 3. The light curves indicate that intranight variability was found on several nights both in B and R bands. The violent intranight variability could be about 0.4 mag on several nights in both bands. Besides rapid variations over timescale of hours, long-term variation could also be found. During the observations of 2010 (corresponding dates on the time-axis of 3667 to 3673), the object was fainter in both two bands. The variations of the source in both bands are similar with each other. The confirmed violent INOV provides strong evidence supporting the fact that SDSS J094857.3+002225 holds a relativistic jet.

5. Discussion

Paliya et al. (2013) used aperture photometry to obtain the light curves of 1H 0323+342 and suggested the existence of INOV in it. Here, for 1H 0323+342, ordinary aperture photometry was also used to estimate the influence of the host galaxy. After the image pre-processing, standard aperture photometry routine of IRAF was used to get the instrumental magnitudes. Several comparison stars from the same frame were selected to get the differential magnitudes as above. The differential magnitude light curves of 1H 0323+342 obtained using this method are plotted in Fig. 4. Although in Fig. 4, 1H 0323+342 seems to show optical variability on several nights, the variation should be checked carefully for the existence of the extended host galaxy. The relation between the differential magnitude obtained through ordinary aperture photometry and the FWHM of

the frames was used to check the variation. It has been found that the aperture photometry differential magnitude is correlative to the FWHM of the frames (Fig. 5 top panels). Thus, the apparent variation gotten through aperture photometry is blended by the variable seeing. The contamination of the host galaxy should be considered during the data analysis of object 1H 0323+342.

As indicated above, the influence of the extended host galaxy of 1H 0323+342 should be considered. Thus, it is significant to make sure whether the influence of host galaxy still remains when the difference image subtraction technique is used. We checked the relation between the image subtraction differential “magnitude” and the FWHM of the frames in Fig. 5 bottom panels. It could be found that there are no distinct correlation between the differential “magnitude” and the FWHM in both two optical bands in the figure. It is confirmed that our method has not been blended by the variable seeing. On the other hand, we used image subtraction method to deal with the archive data of SDSS J094857.3+002225 used in the letter of Liu et al. (2010) to check the effectiveness of the method. SDSS J094857.3+002225 is a point-like source without extended host galaxy. We used its high quality data obtained on the night of 2009 March 1. The differential “magnitude” light curves of SDSS J094857.3+002225 are plotted in Fig. 6. The visible variability of the object on both two bands could be easily found in Fig. 6. The curves were consistent to those shown in the work by Liu et al. (2010), although its signal-to-noise ratio is lower than those obtained with aperture photometry. At the same time, the differential “magnitude” fluctuations of the comparison stars were small. It is similar to the result shown in figure 6 by Choi et al. (2014). It demonstrates that the image subtraction method could reveal the actual variability of object.

6. Conclusions

We observed the γ -ray NLS1 1H 0323+342 in optical B and R bands using the NAOC 2.16 m telescope. Image subtraction technique was used to deal with the observation data because of the existence of extended host galaxy. Then residual fluxes were obtained using aperture photometry from difference images. It has been found that the intranight fluctuations of the object are comparable to those of check stars with steady intrinsic brightness. On the day timescale, 1H 0323+342 has been detected variable in our observations. It is indicated that variability on day timescale has been found in 1H 0323+342, although no significant intranight optical variability has been detected in our observations. The variability on day timescale provides evidence supporting the existence of a relativistic jet in 1H 0323+342. The first γ -ray detected NLS1 SDSS J094857.3+002225 was monitored by the 80 cm TNT telescope in optical band. The observations confirm the presence of INOV in both B and R bands. This indicates the existence of relativistic jet in the object with a small viewing angle.

Our work also suggested that the difference image subtraction technique could be used to obtain the light curves of AGN even when images were blended with extended host galaxy, while the ordinary aperture photometry would not be adopted. It is suggested that the difference image subtraction technique is effective to reveal the variation.

The origin of the different optical variation properties between these two γ -ray NLS1s are still not clear. More information, farther multiwavelength monitoring with denser sampling rate and high quality radio mapping are needed to understand the differences.

Acknowledgments

The work is supported by the National Basic Research Program of China (973-program, grant 2014CB845800) and by the

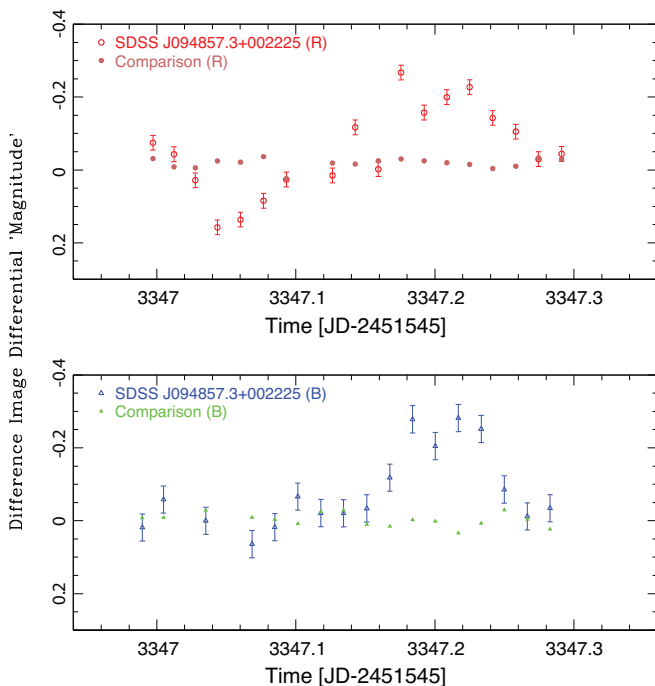


Fig. 6. Difference image “magnitude” curves of SDSS J094857.3+002225 acquired through image subtraction method. The top panel gives light curves obtained using the archive data on the night of 2009 March 1 in R band. The red open circles and pink filled circles represent the difference image differential “magnitude” of SDSS J094857.3+002225 and comparison star in R band, respectively. The bottom panel gives light curves obtained using the archive data on the same night in B band. The blue open triangles and green filled triangles represent the difference image differential “magnitude” of SDSS J094857.3+002225 and comparison star in B band, respectively. (For interpretation of the references to colour in this figure legend, the reader is referred to the web version of this article).

National Science Foundation of China through grant 11273027, 11473036 and U1431108.

References

- Abdo, A.A., et al., 2009a. *ApJ* 699, 976.
- Abdo, A.A., et al., 2009b. *ApJ* 707, 727.
- Abdo, A.A., et al., 2009c. *ApJL* 707, L142.
- Alard, C., 2000. *A&AS* 144, 363.
- Alard, C., Lupton, R.H., 1998. *ApJ* 503, 325.
- Antón, S., Browne, W.A., Marchã, M.J., 2008. *A&A* 490, 583.
- Blandford, R.D., Payne, D.G., 1982. *MNRAS* 199, 883.
- Blandford, R.D., Znajek, R.L., 1977. *MNRAS* 179, 433.
- Boller, T., 1997. *Astron. Nachr.* 318, 209.
- Boller, T., Brandt, W.N., Fink, H., 1996. *A&A* 305, 53.
- Boroson, T.A., 2002. *ApJ* 565, 78.
- Calderone, G., 2011. *MNRAS* 413, 2365.
- Choi, Y., 2014. *ApJ* 782, 37.
- Collin, S., Kawaguchi, T., 2004. *A&A* 426, 797.
- Doi, A., Nagira, H., Kawakatu, N., 2012. *ApJ* 760, 41.
- Eggen, J.R., Maune, J.D., Miller, H.R., 2014. arXiv:1404.5355
- Eggen, J.R., Miller, H.R., Maune, J.D., 2013. *ApJ* 773, 85.
- Foschini, L., et al., 2011. In: Foschini, L., Colpi, M., Gallo, L., et al. (Eds.), in *Narrow-Line Seyfert 1 Galaxies and Their Place in the Universe*. (Trieste: PoS), 024
- Foschini, L., 2012. *A&A* 548, A106.
- Foschini, L., Fermi/LAT Collaboration, Ghisellini, G., et al., 2010. (LAT Collaboration). In: Maraschi, L., Ghisellini, G., Ceca, R.D., Tavecchio, F., et al. (Eds.), *Accretion and Ejection in AGN: a Global View*, 427. Fermi/LAT Collaboration, p. 243. *ASP Conf. Ser.*
- Foschini, L., Maraschi, L., Tavecchio, F., Ghisellini, G., Gliozzi, M., Sambruna, R.M., 2009. *Adv. Space Res.* 43, 889.
- Gallo, L.C., Edwards, P.G., Ferrero, E., 2006. *MNRAS* 370, 245.
- Goodrich, R.W., 1989. *ApJ* 342, 224.
- Greene, J.E., Ho, L.C., Ulvestad, J.S., 2006. *ApJ* 636, 56.
- Grupe, D., Mathur, S., 2004. *ApJL* 606, L41.
- Healey, S.E., Romani, R.W., Taylor, G.B., Sadler, E.M., Ricci, R., Murphy, T., Ulvestad, J.S., Winn, J.N., 2007. *ApJS* 171, 61.
- Heinzeller, D., Duschl, W.J., 2007. *MNRAS* 374, 1146.
- Ho, L.C., 2002. *ApJ* 564, 120.
- Huang, F., Li, J., Wang, X., 2012. *RAA* 12, 1585.
- Ikejiri, Y., Uemura, M., Sasada, M., 2011. *PASJ* 63, 639.
- Itoh, R., Tanaka, Y.T., Fukazawa, Y., 2013. *ApJL* 775, L26.
- Jang, M., Miller, H.R., 1997. *AJ* 114, 565.
- Kellermann, K.I., Sramek, R., Schmidt, M., Shaffer, D.B., Green, R., 1989. *AJ* 98, 1195.
- Komossa, S., Voges, W., Xu, D., Mathur, S., Adorf, H.M., Lemson, G., Duschl, W., Grupe, D., 2006. *AJ* 132, 531.
- Laor, A., 2000. *ApJL* 543, L111.
- Leighly, K.M., 1999. *ApJS* 125, 297.
- León Tavares, J., Kotilainen, J., Chavushyan, V., 2014. *ApJ* 795, 58.
- Liu, H., Wang, J., Mao, Y., Wei, J., 2010. *ApJL* 715, L113.
- Malizia, A., Bassani, L., Bird, A.J., 2008. *MNRAS* 389, 1360.
- Mathur, S., Grupe, D., 2005. *A&A* 432, 463.
- Maune, J.D., Miller, H.R., Eggen, J.R., et al., 2011. In: Foschini, L., Colpi, M., Gallo, L., et al. (Eds.), in *Narrow-Line Seyfert 1 Galaxies and Their Place in the Universe*. (Trieste: PoS), 002
- Maune, J.D., Miller, H.R., Eggen, J.R., 2013. *ApJ* 762, 124.
- Neumann, M., Reich, W., Fuerst, E., et al., 1994. *A&AS* 106, 303.
- Osterbrock, D.E., Pogge, R.W., 1985. *ApJ* 297, 166.
- Padovani, P., Costamante, L., Ghisellini, G., Giommi, P., Perlmutter, E., 2002. *ApJ* 581, 895.
- Paliya, V.S., 2013. *MNRAS* 428, 2450.
- Paliya, V.S., 2014. *ApJ* 789, 143.
- Paliya, V.S., Stalin, C.S., Ravikumar, C.D., 2015. *AJ* 149, 41.
- Panessa, F., 2011. *MNRAS* 417, 2426.
- Pogge, R.W., 2000. *New Astron. Rev.* 44, 381.
- Remillard, R.A., Grossan, B., Bradt, H.V., Ohashi, T., Hayashida, K., 1991. *Natur* 350, 589.
- Sikora, M., Stawarz, Ł., Lasota, J.-P., 2007. *ApJ* 658, 815.
- Stalin, C.S., Gopal-Krishna R., Sagar, Wiita, P.J., 2004. *MNRAS* 350, 175.
- Véron-Cetty, M.-P., Véron, P., 2010. *A&A* 518, A10.
- Wagner, S.J., Witzel, A., 1995. *Annu. Rev. Astron. Astrophys.* 33, 163.
- Wajima, K., Fujisawa, K., Hayashida, M., 2014. *ApJ* 781, 75.
- Wang, T.G., Matsuoka, M., Kubo, H., Mihara, T., Negoro, H., 2001. *ApJ* 554, 233.
- Webb, W., Malkan, M., 2000. *ApJ* 540, 652.
- Whalen, D.J., Laurent-Muehleisen, S.A., Moran, E.C., Becker, R.H., 2006. *AJ* 131, 1948.
- Yao, B., Huang, L., 2002. *ChJAA* 2, 563.
- Yao, S., Yuan, W., Komossa, S., 2015. *AJ* 150, 23.
- Yuan, W., Zhou, H.Y., Komossa, S., Dong, X.B., Wang, T.G., Lu, H.L., Bai, J.M., 2008. *ApJ* 685, 801.
- Zhou, H., 2007a. *ApJL* 658, L13.
- Zhou, H.Y., 2007b. *ApJS* 166, 128.
- Zhou, H.-Y., Wang, T.-G., 2002. *ChJAA* 2, 501.
- Zhou, H.-Y., Wang, T.-G., Dong, X.-B., Li, C., Zhang, X.-G., 2005. *ChJAA* 5, 41.
- Zhou, H.Y., Wang, T.G., Dong, X.B., Zhou, Y.Y., Li, C., 2003. *ApJ* 584, 147.